Mean field and pairing properties in the crust of neutron stars

F. Montani
Institut d' Astronomie et d' Astrophysique, Universite Libre de Bruxelles, Campus de la Plaine Code Postal 226, Boulevard du Triomphe, B-1000 Brussels, Belgium

C. May and H. Müther
Institut für Theoretische Physik, Universität Tübingen, D-72076 Tübingen, Germany
(Received 12 January 2004; published 11 June 2004)

Properties of the matter in the inner crust of a neutron star are investigated in a Hartree-Fock plus BCS approximation employing schematic effective forces of the type of the Skyrme forces. Special attention is paid to differences between a homogenous and inhomogeneous description of the matter distribution. For that purpose self-consistent Hartree-Fock calculations are performed in a spherical Wigner-Seitz cell. The results are compared to predictions of corresponding Thomas-Fermi calculations. The influence of the shell structure on the formation of pairing correlations in inhomogeneous matter are discussed.

DOI: 10.1103/PhysRevC.69.065801 PACS number(s): 26.60.+c, 21.60.Jz

I. INTRODUCTION

The determination of the equation of state (EoS) for nucleon matter is an important ingredient for various investigations of astrophysical objects. A lot of attention has been paid to the EoS of baryonic matter at densities above the saturation density of nuclear matter ($\rho_0 \approx 0.16$ fm^{-3}). These densities should be relevant to describing the interior of neutron stars and are of particular interest, as they give rise to speculations about exotic phases of baryonic matter including the existence of kaon condensates or quark matter [1–3].

However, it is not only this regime of very high densities that is interesting, but also the crust of neutron stars should be a very intriguing phase of baryonic matter. At those lower densities and low temperatures the free energy should be reduced by allowing for a phase of inhomogeneous baryonic matter. This nonuniform matter should consist of a lattice of quasinuclei embedded in a gas of electrons and possibly also a sea of neutrons. Thomas-Fermi calculations, which are based on nonrelativistic or relativistic mean-field calculations for the homogenous system, exhibit these features [4–8].

The presence of neutron superfluidity in the crust of neutron stars seems to be well established. This is based on investigations solving the BCS gap equation in homogenous nuclear matter [9–12] . The precise knowledge of the pairing gap is very important for the determination of the cooling rate of neutron stars. The superfluidity of the material of the crust should have a significant influence on the rotation frequencies of the star. The formation of glitches may be related to the vortex pinning of the superfluid phase in the inhomogeneous crust.

The aim of the investigations presented in this paper is to explore the basic properties of this inhomogeneous phase of baryonic matter on a level beyond the Thomas-Fermi approximation. What are the consequences of shell effects in the quasinuclei in the systems for the bulk properties of this material? How do they influence the proton fraction in the β equilibrium? What are the consequences of these quasinuclei on the pairing properties of the system?

To answer these questions we perform nuclear structure calculations in a Wigner-Seitz cell of spherical shape. The assumption of such a spherical cell is not designed to allow for inhomogeneities of the matter, which is different from the formation of quasinuclei or bubbles in the homogenous matter. Therefore we do not consider a formation of rods or slabs of increased density [8]. Also at this stage, we do not aim at a complete survey of this matter covering a large region of various densities. Instead we wish to explore some features of nuclear structure calculations beyond the Thomas-Fermi approach for a few selected examples.

For that purpose we perform Hartree-Fock (HF) and HF plus BCS calculations in an appropriate basis of the spherical Wigner-Seitz cell. For the *NN* interaction we use rather simple effective forces of the Skyrme type [13,14]. Special attention is paid to the pairing gaps resulting from calculations of the homogenous matter and the nonhomogeneous system.

After this Introduction we discuss in Sec. II the techniques and results of HF calculations for the β-stable matter within a spherical Wigner-Seitz cell. The determination of pairing properties is presented in Sec. III, which is followed by a short summary and conclusions in Sec. IV.

II. HF CALCULATIONS IN A SPHERICAL BOX

The single-particle wave functions for the nucleon considered in our calculations are expanded in a complete basis of orthonormal states defined within a spherical box of radius R. Such an orthonormal set of basis functions, which are regular at the origin in the center of the box, is given by

$$\Phi_{iljm}(\vec{r}) = \langle \vec{r} | iljm \rangle = R_{il}(r) \mathcal{Y}_{ljm}(\vartheta, \varphi). \tag{1}$$

In this equation $\mathcal{Y}_{ljm}$ represent the spherical harmonics including the spin degrees of freedom by coupling the orbital angular momentum l with the spin to a single-particle angular momentum j. The radial wave functions R_{il} are given by the spherical Bessel functions, $R_{il}(r) \sim j_l(k_i r)$ for the discrete momenta k_i, which fulfill

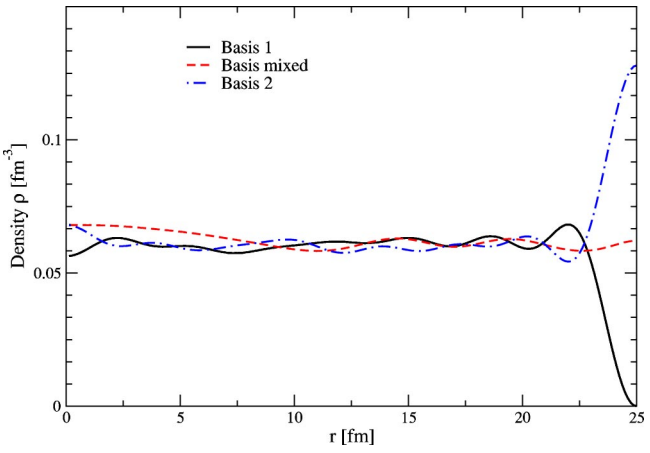

FIG. 1. (Color online) The local density for homogeneous matter (ρ=0.06 fm^{-3}) calculated according to Eq. (5) using Basis 1 (2), Basis 2 (6), and the mixed basis as described in the text.

$$R_{il}(R) = N_{il} j_l(k_i R) = 0. \tag{2}$$

The normalization constant

$$N_{il} = \begin{cases} \dfrac{\sqrt{2}}{\sqrt{R^3} j_{l-1}(k_i R)} & \text{for } l > 0, \\ \dfrac{i\pi\sqrt{2}}{\sqrt{R^3}} & \text{for } l = 0, \end{cases} \tag{3}$$

ensures that the basis functions are orthogonal and normalized within the box,

$$\int_0^R d^3 r \Phi^*_{iljm}(\vec{r}) \Phi_{i'l'j'm'}(\vec{r}) = \delta_{ii'} \delta_{ll'} \delta_{jj'} \delta_{mm'}. \tag{4}$$

Adopting this basis of eigenstates for the kinetic energy one can try to describe homogenous nuclear matter with a constant density ρ_π and ρ_ν for protons and neutrons, respectively, by filling all basis states with momenta k_i below the corresponding Fermi momentum k_{F_π} and k_{F_ν}. The local density is then given by

$$\rho(r) = \sum_{ilj} \Theta(k_F - k_i)(2j+1) R^2_{il}(r), \tag{5}$$

where Θ stands for the Heaviside function. The results for this local density considering a spherical box with the radius R=25 fm, and trying to describe a system with a density of 0.06 fm^{-3}, are displayed in Fig. 1. From this figure one can see that the local density is in reasonable agreement with the mean value, except at the border of the cavity at $r=R$. Since all wave functions by construction are bound to disappear at this borderline, the same is also true for the density.

In order to cure this deficiency one could try an alternative basis for the radial functions by the boundary condition that the radial derivative vanishes at the surface of the box

$$\widetilde{R}_{il}(r) = \widetilde{N}_{il} j_l(\widetilde{k}_i r) \text{ with } \frac{\partial \widetilde{R}_{il}}{\partial r}(R) = 0. \tag{6}$$

So all these basis function exhibit an extremum at the surface of the Wigner-Seitz cell, which leads to a maximum of the local density at $r=R$ if these functions are employed in Eq. (5), as one can see from the curve labeled "Basis 2" in Fig. 1.

Bonche and Vautherin [15] suggested to use a mixed basis by employing, e.g., basis states with the boundary condition (2) for states with even l and those with the boundary condition (6) for states with odd orbital angular momentum l. This recipe cures the deviation of the local density from the mean value at the surface (see also Fig. 1). Nevertheless, the representation of the homogenous phase of nuclear matter within a spherical box of finite size leads to slight fluctuations in the local density. Furthermore, one must be aware of shell effects, which are due to the finite size of the spherical box considered.

In order to explore the influence of these shell effects on the evaluation of expectation values, we have considered spherical boxes of various radii and calculated the binding energy per nucleon for homogenous nuclear matter using the representation of the plane-wave states discussed above. We have considered values for the radius R ranging from 15 to 25 fm. Most of the results turned out to be rather insensitive to the choice of the basis [Eqs. (2) and (6), or mixture]. Therefore, if not stated differently, we will present results for the basis (2) only.

As a first example we consider the homogenous system of neutrons, protons, and electrons in β equilibrium. This means that for any value of the baryon density considered,

$$\rho = \rho_\pi + \rho_\nu, \tag{7}$$

we determine the proton abundance

$$Y_\pi = \frac{\rho_\pi}{\rho}, \tag{8}$$

by the requirement that the Fermi energy for the neutrons is identical to the Fermi energy of the protons plus the Fermi energy of the electrons with the density of electrons being identical to the density of protons.

The results for the energy per nucleon and the proton abundance are displayed in Figs. 2 and 3, respectively. For the range of densities considered, the results obtained in the spherical boxes of different size agree rather well with the corresponding observables calculated in the infinite system. A significant discrepancy is only observed in the calculation of the total energy at higher densities considering boxes with small radii. In these cases the surface effects displayed in Fig. 1, as well as the shell effects, lead to energies which are too small as compared to the result for the infinite system.

After this test of the box basis to describe the homogenous system, we now turn to the HF description within such a spherical box. The HF single-particle wave functions are expanded in the basis of Eq. (1) by

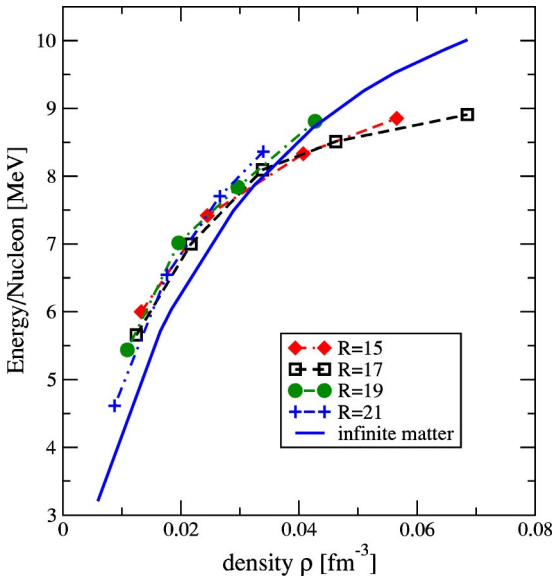

FIG. 2. (Color online) Energy per nucleon for homogenous matter in β equilibrium. The results for infinite matter are compared to those obtained in spherical boxes of different radii. The Skyrme I has been used for the *NN* interaction.

$$\Psi_{\alpha ljm}(\vec{r}) = \sum_{i=1}^{N} c_{\alpha ilj} \Phi_{iljm}(\vec{r}). \tag{9}$$

The number of basis states N is chosen to guarantee that the results are not affected by this limitation. The results of self-consistent HF calculations are displayed in Fig. 4, showing the density of protons and neutrons as a function of the radial distance from the center of a box with the radius R=21 fm. The particle numbers for protons (Z=20 in this example) and neutrons (N=388) have been determined to fulfill the condition of β stability, employing the Fermi energies evaluated in the HF calculation.

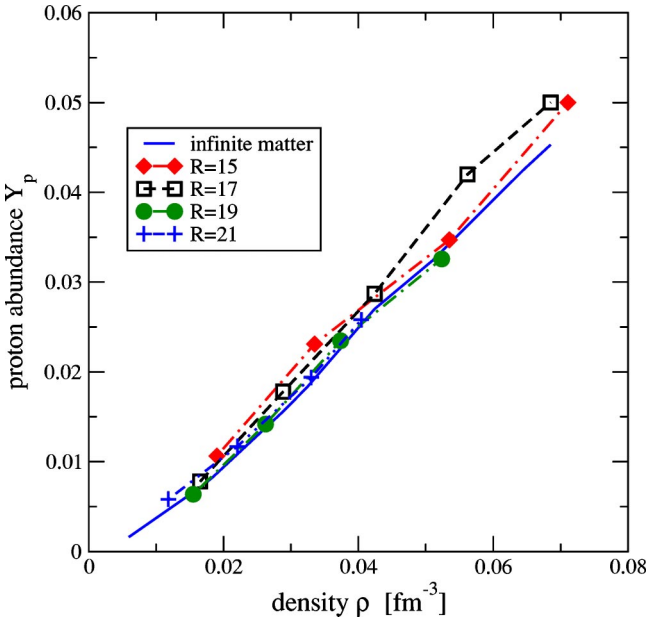

FIG. 3. (Color online) Proton abundance Y_p for homogenous matter in β equilibrium. For further comments, see Fig. 2.

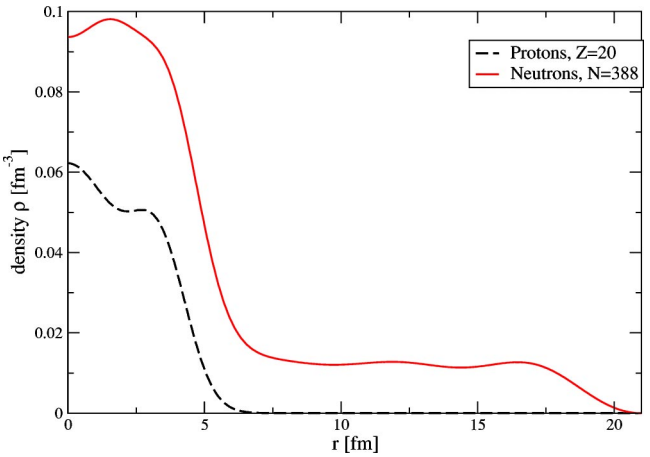

FIG. 4. (Color online) Density distributions derived from HF calculations for nuclear matter in β equilibrium.

The density distribution for the protons is different from zero only near the center of the Wigner-Seitz cell. In this region also the density of the neutrons is considerably larger than in the rest of the spherical box. Therefore, we can interpret this configuration as a quasinucleus embedded in a neutron see. The single-particle energy spectrum for the protons exhibit a clear shell structure up to energies around the Fermi energy. The density of states around the corresponding Fermi energy is larger for the neutrons. In fact, it is close to the one of the homogeneous matter described in the spherical box of this size.

For the example of Z=20 protons and N=388 neutrons in a Wigner-Seitz cell with the radius R=21 fm considered in Fig. 4, we obtain a global density of ρ=0.0105 fm^{-3} and an abundance for the protons of Y_p=0.049. The energy per nucleon for this self-consistent solution of the HF equations is about 2 MeV per nucleon below the energy which was obtained for the homogenous distribution of matter in β equilibrium.

Figure 5 exhibits this gain in energy due to the formation of quasinuclei in β-stable nuclear matter. For small densities around ρ=0.01 fm^{-3} the HF solution with localized quasinuclei yields an energy which is about 3 MeV per nucleon below the energy of the corresponding homogenous matter. This gain in energy decreases with increasing density to around 1 MeV per nucleon at ρ=0.04 fm^{-3}. The results are rather independent on the size of the Wigner-Seitz cell under consideration.

The HF calculations allowing for an inhomogeneous distribution of matter, however, also yield different results for the proton abundances as compared to the results obtained for homogenous nuclear matter in β equilibrium (see Fig. 6). Thomas-Fermi calculation, which allow for an inhomogeneous distribution of matter, show proton abundances which are slightly above those derived from the calculation of homogenous matter. This indicates that the fluctuations in the density, which are taken into account in the Thomas-Fermi calculations, tend to enhance the proton abundances, as regions with high densities contain a larger fraction of protons.

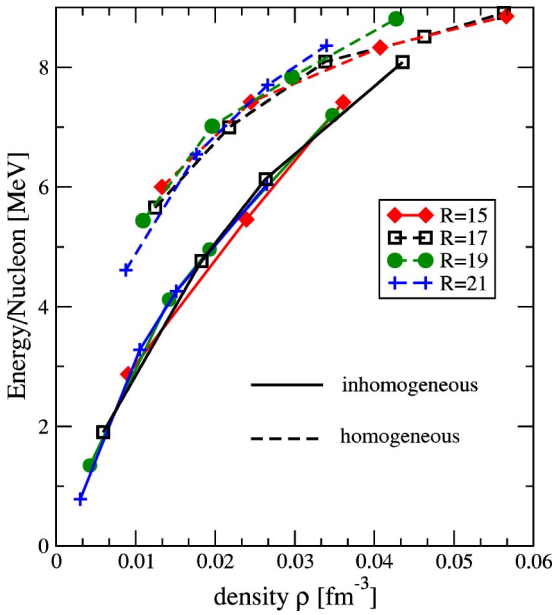

FIG. 5. (Color online) Energy per nucleon of β-stable nuclear matter in the homogenous phase (symbols connected by dashed line) and inhomogeneous phase (symbols connected by solid line).

However, the main effect in the enhancement of the proton abundances observed in the HF approach is not described by the Thomas-Fermi model. It originates from the pronounced shell structure of the proton single-particle energies. The HF calculation favors distributions of matter with a quasinucleus showing a closed shell for the protons.

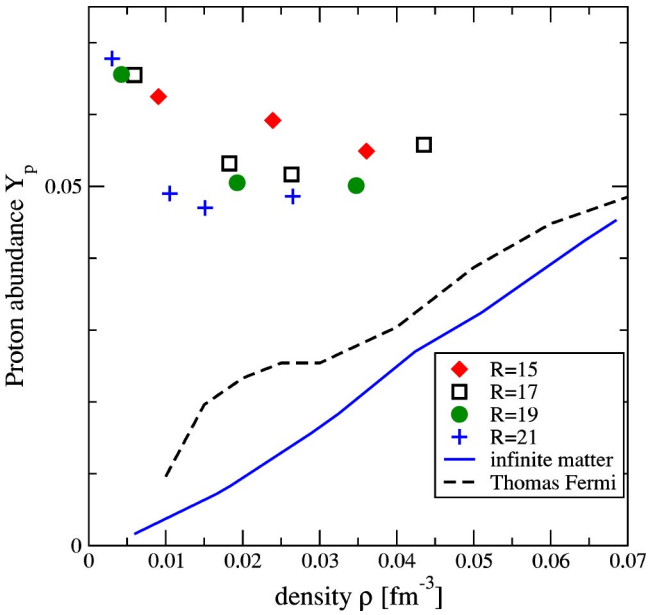

FIG. 6. (Color online) Proton abundances of β-stable nuclear matter in the homogenous case of homogenous infinite matter (solid line), inhomogeneous matter determined in the Thomas-Fermi approximation, and in HF calculations employing Wigner-Seitz cells of different radii.

III. PAIRING IN THE CRUST OF NEUTRON STARS

After we have noticed the effects of shell structure on the decomposition of the nuclear material, we would like to address in this section the question of how this shell structure can affect the pairing properties of the nuclear material. In particular, we consider neutron-neutron pairing for neutron pairs with a total momentum equal to zero in a $^1S_0$ partial wave for the relative motion. Using the standard BCS approach for homogenous matter, the pairing gap $\Delta(k)$ for a pair of neutrons with relative momentum $k=|\vec{k}|$ is obtained by solving the gap equation [9,11,12]

$$\Delta(k) = -\frac{2}{\pi}\int_0^\infty dk' k'^2 V(k,k') \frac{\Delta(k')}{2\sqrt{(\varepsilon_k' - \varepsilon_F)^2 + \Delta(k')^2}}. \tag{10}$$

Here $V(k,k')$ denotes the matrix elements of the NN interaction in the $^1S_0$ partial wave, ε_k the single-particle energy for a nucleon with momentum k, and ε_F the Fermi energy. Instead of using the matrix elements for a realistic NN interaction which is fitted to the NN scattering data, we have chosen to employ an effective interaction which is of zero range, density dependent, and has been proposed by Bertsch and Esbensen [16,17],

$$V(r_1,r_2) = v_0\left[1 - \eta\left(\frac{\rho(r_1)}{\rho_0}\right)^\alpha\right]\delta(r_1 - r_2), \tag{11}$$

where v_0, η, and α are adjustable parameters and ρ_0 is the saturation density of nuclear matter. For such a zero-range interaction a cutoff parameter ε_C must be introduced in the gap equation to truncate the integral to states with energy ε_k less than ε_C. These four parameters can be constrained to reproduce the NN scattering length and Garrido *et al.* [18] determined various sets of parameters which reproduce pairing gaps for nuclear and neutron matter calculated with realistic NN interactions. We used the parameters v_0 =481 MeV fm^3, η=0.45, α=0.47, and ε_C=60 MeV and verified that this set of parameters leads to pairing gaps for homogenous neutron matter, which are in fair agreement with those evaluated for the CD Bonn interaction [19].

We now turn to the solution of the HF+BCS equations [20], which in the spherical Wigner-Seitz cells have the form

$$\begin{aligned}(\varepsilon_{nlj} - \varepsilon_F)u_{nlj} + \Delta_{nlj}v_{nlj} &= E_{nlj}u_{nlj},\\ -(\varepsilon_{nlj} - \varepsilon_F)v_{nlj} + \Delta_{nlj}u_{nlj} &= E_{nlj}v_{nlj},\end{aligned} \tag{12}$$

where

$$E_{nlj} = \sqrt{(\varepsilon_{nlj} - \varepsilon_F)^2 + \Delta_{nlj}^2},$$

is the energy of the quasiparticle state with quantum numbers n,l, and j and ε_{nlj} the corresponding single-particle energy determined in the HF equations. From the coefficients u_{nlj}, v_{nlj}, and the corresponding single-particle wave functions Ψ_{nljm} [see Eq. (9)], one can calculate the anomalous density

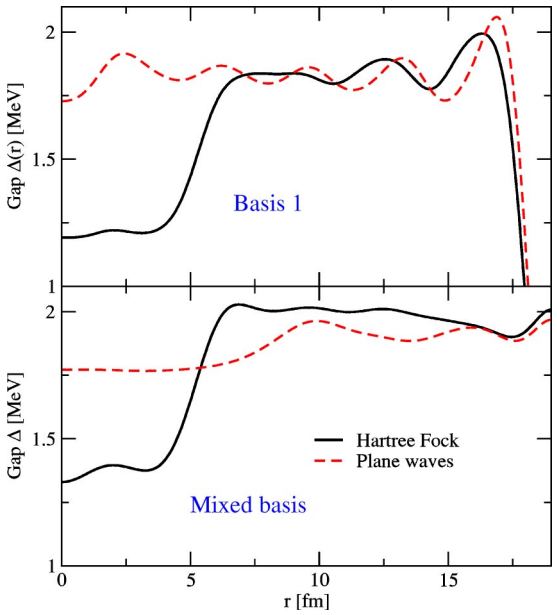

FIG. 7. (Color online) Local gap function $\Delta(r)$ as defined in Eq. (15) for β-stable matter of density $\rho=0.02$ fm^{-3}. The results are displayed for the plane wave plus BCS approach (dashed line) and the HF plus BCS approach (solid line). While the upper panel exhibits the results obtained in Basis 1 [see Eq. (2)], the lower part of the figure displays the results obtained for the mixed basis.

$$\chi(r) = \sum_{nlj} (2j+1) \frac{u_{nlj} v_{nlj}}{2} \Psi^2_{nlj}(r), \tag{13}$$

and the expression for the normal density is changed into

$$\rho(r) = \sum_{nlj} (2j+1) v^2_{nlj} \Psi^2_{nlj}(r). \tag{14}$$

Using an interaction of zero range, like Eq. (11) does, leads to a definition of a local gap function

$$\Delta(r) = V(r)\chi(r), \tag{15}$$

from which one can calculate the state-dependent pairing gaps

$$\Delta_{nlj} = \int \Delta(r) \Psi^2_{nlj}(r) r^2 dr. \tag{16}$$

The BCS equations (12)–(16) have to be solved together with the HF equations in a self-consistent way. The Fermi energy ε_F is adjusted to reproduce the requested particle numbers or densities for protons and neutrons. These equations can be reduced to an approach, which we will call BCS with plane waves in the spherical box, by restricting the radial wave functions for the single-particle states to the spherical Bessel functions defined in Eq. (2) or Eq. (6).

The results for the gap function $\Delta(r)$ defined in Eq. (15) for β-stable matter of a density $\rho=0.02$ fm^{-3} are displayed in Fig. 7. The gap function evaluated for the plane-wave basis are presented by the dashed line. We find that this gap function fluctuates around 1.8 MeV with a sharp drop at the boundary of the spherical box. This drop is of course related

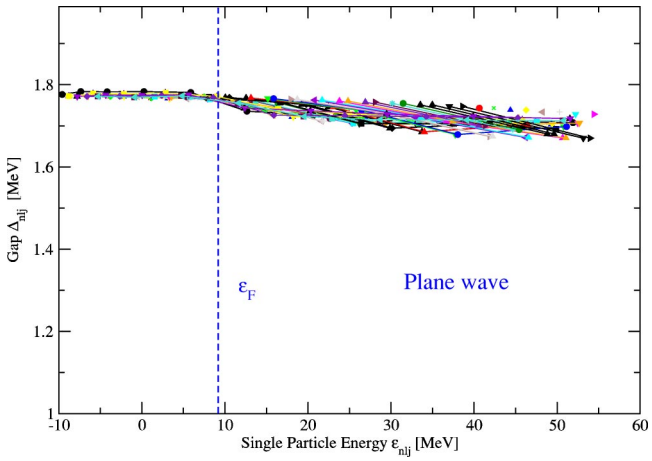

FIG. 8. (Color online) The results for the state-dependent pairing gaps Δ_{nlj} defined in Eq. (16) for β-stable matter of density $\rho=0.02$ fm^{-3} as derived from plane wave plus BCS calculation. These gaps are displayed as a function of the corresponding ε_{nlj}. Each gap is presented by a symbol, and gaps belonging to states with identical orbital angular momentum l and angular momentum j are connected by a line.

to the boundary condition (2) of all wave functions. As already discussed for the local density above, this deficiency can be cured by using a mixed basis, switching between Eqs. (2) and (6) for states with even and odd parity (see lower panel of Fig. 7).

Solving the BCS plus HF equations, one obtains a gap function with values which are suppressed by about 25% in the area of the quasinuclei. From this result one may speculate that the inhomogeneous matter leads to regions of enhanced densities in which the formation of pairing correlations is suppressed to some extent. Therefore, these regions might be considered as nuclei for the formation of normal matter within the superfluid phase of neutron matter. Also one could imagine that these quasinuclei could lead to vortex pinning in the rotation of the superfluid crust of neutron stars.

This observation would be in agreement with the results for the pairing gap derived in a local density approximation (LDA) as one can see, e.g., from Fig. 4 of [21]. In this paper Barranco *et al.* demonstrate that that the LDA is not a very good approximation and account for the nonlocality of the pairing correlations by determining a momentum dependent gap. These calculations are based on single-particle states determined from a Woods-Saxon potential and lead to gap functions which depend only weakly on the position.

This indicates that a more detailed analysis of the pairing correlation may be required for an inhomgenous system (see also [22]). Therefore, we are going to study the state-dependent gaps Δ_{nlj} displayed in Figs. 8 and 9 for the plane wave plus BCS and HF plus BCS calculations, respectively. It should be kept in mind that many properties of the system, like the specific heat or the response functions at low energies (which are relevant, e.g., for the propagation of neutrinos), are very sensitive to the quasiparticle energies around the Fermi energy, which means that they are sensitive to the gap for states close to the Fermi energy.

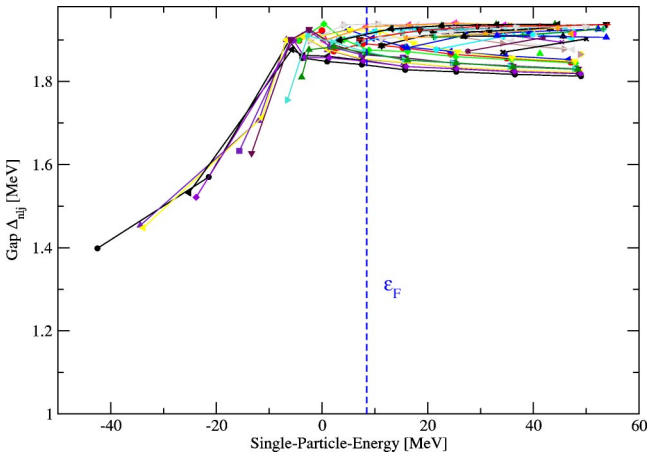

FIG. 9. (Color online) Results for the state-dependent pairing gaps Δ_{nlj} as derived from a HF plus BCS calculation. For further details, see Fig. 8.

Comparing the results displayed in Figs. 8 and 9 it is not so important to disentangle details but to observe the general trends for the gaps as a function of the underlying single-particle energy. One finds that the homogenous system, which is described in terms of the plane wave plus BCS calculation, leads to a gap Δ_{nlj}, which is almost independent of the state.

The calculation of the inhomogeneous system, on the other hand, leads to a few single-particle states, which are much more bound than the lowest states in the homogeneous calculation (−42 MeV as compared to −9.5 MeV). These deeply bound states are localized near the origin. This large binding of the single-particle states which leads to a reduction of the density of states is also responsible for the reduction of the pairing gap for these low-lying states. On the other hand, the states with single-particle energies close to the Fermi energy ε_F show a value for the gap parameter which is very close to the one derived for the homogenous system.

This implies that the reduction of the gap function $\Delta(r)$ in the region of the quasinuclei discussed above manifests itself mainly in a reduction of the pairing gap for the deeply bound single-particle states. The evaluation of response functions and other observables, however, is in general sensitive to the gap at the Fermi energy. Therefore, one cannot expect major differences in the behavior of the inhomogeneous, as compared to the homogeneous, system of matter with respect to the pairing properties of the neutrons. This shall be different for smaller densities, where the Fermi energy for the neutrons drops to values at which the shell structure of the single-particle energies is significant.

IV. CONCLUSIONS

The transition from homogenous to inhomogeneous matter as it occurs in the crust of neutron stars has been investigated. Special attention has been paid to the consequences of shell effects, which occur assuming a phase of quasinuclei embedded in a sea of neutrons. For that purpose, HF plus BCS calculations are performed assuming a basis of single-particle states for a spherical Wigner-Seitz cell. It is observed that the shell effects lead to a substantial increase for the proton abundance in β-stable baryonic matter.

Shell effects are also responsible for a decrease of the localized pairing gap in the region of the quasinuclei. A more detailed analysis, however, shows that this reduction of the local gap function $\Delta(r)$ is mainly due to a reduction of the pairing gap for the deeply bound single-particle states. The pairing properties for the single-particle states close to the Fermi energy are similar to those obtained for a homogenous description of the system.

The present studies are based on simple parameterizations for the effective *NN* interaction. It may be of interest to study whether the predictions for the transition from homogenous to inhomogeneous matter also hold, when more realistic *NN* interactions are employed.

The use of a spherical Wigner-Seitz cell is a source of various deficiencies. The boundary conditions at the border of the cell lead to fluctuations in the density, which complicate the comparison with the infinite homogenous system. This could be improved by employing a Cartesian basis, which is more involved from the numerical point of view. The use of a Cartesian basis, however, would also allow for the study of nonspherical structures.

ACKNOWLEDGMENTS

We would like to thank Stephane Goriely, Mike Pearson, and Mathieu Samyn for very helpful discussions. One of us (F.M.) was supported by a stipend of the "Deutsche Akademische Austauschdienst" (DAAD, Germany). This financial support is also gratefully acknowledged.

[1] M. Prakash, I. Bombaci, M. Prakash, P. J. Ellis, J. M. Lattimer, and R. Knorren, Phys. Rep. **280**, 1 (1997).
[2] H. Heiselberg and M. Hjorth-Jensen, Phys. Rep. **328**, 237 (2000).
[3] S. Pal, M. Hanauske, I. Zakout, H. Stocker, and W. Greiner, Phys. Rev. C **60**, 015802 (1999).
[4] K. Oyamatsu, Nucl. Phys. **A561**, 431 (1993).
[5] K. Sumiyoshi, K. Oyamatsu, and H. Toki, Nucl. Phys. **A595**, 327 (1995).
[6] H. Shen, Phys. Rev. C **65**, 035802 (2002).
[7] M. Pi, X. Vinas, M. Barranco, A. Perez-Canyellas, and A. Polls, Astron. Astrophys., Suppl. Ser. **64**, 439 (1986).
[8] G. Watanabe, K. Iida, and K. Sato, Nucl. Phys. **A676**, 455 (2000).
[9] M. Baldo, J. Cugnon, A. Lejeune, and U. Lombardo, Nucl. Phys. **A515**, 409 (1990).
[10] V. A. Kodel, V. V. Kodel, and J. W. Clark, Nucl. Phys. **A598**, 390 (1996).

[11] Ø. Elgarøy and M. Hjorth-Jensen, Phys. Rev. C **57**, 1174 (1998).
[12] J. Kuckei, F. Montani, H. Müther, and A. Sedrakian, Nucl. Phys. **A723**, 32 (2003).
[13] T. H. R. Skyrme, Nucl. Phys. **9**, 615 (1959).
[14] D. Vautherin and D. M. Brink, Phys. Rev. C **5**, 626 (1972).
[15] P. Bonche and D. Vautherin, Nucl. Phys. **A372**, 496 (1981).
[16] G. F. Bertsch and H. Esbensen, Ann. Phys. (N.Y.) **209**, 327 (1991).
[17] H. Esbensen, G. F. Bertsch, and K. Hencken, Phys. Rev. C **56**, 3054 (1997).
[18] E. Garrido, P. Sarriguren, E. Moya de Guerra, and P. Schuck, Phys. Rev. C **60**, 064312 (1999).
[19] R. Machleidt, Phys. Rev. C **63**, 024001 (2001).
[20] P. Ring and P. Schuck, *The Nuclear Many Body Problem* (Springer, New York, 1980).
[21] F. Barranco, R. A. Broglia, H. Esbensen, and E. Vigezzi, Phys. Rev. C **58**, 1257 (1998).
[22] F. Barranco, R. A. Broglia, H. Esbensen, and E. Vigezzi, Phys. Lett. B **390**, 13 (1997).